A Case for Reverse Protonation: Identification of Glu160 as an Acid/Base Catalyst in *Thermoanaerobacterium saccharolyticum* β-Xylosidase and Detailed Kinetic Analysis of a Site-Directed Mutant†

David J. Vocadlo, Jacqueline Wicki, Karen Rupitz, and Stephen G. Withers*

Protein Engineering Network of Centres of Excellence of Canada and Department of Chemistry, University of British Columbia, Vancouver, British Columbia, Canada V6T 1Z1

Received January 24, 2002; Revised Manuscript Received May 8, 2002

ABSTRACT: The catalytic mechanism of the family 39 *Thermoanaerobacterium saccharolyticum* β-xylosidase (XynB) involves a two-step double-displacement mechanism in which a covalent α-xylosyl−enzyme intermediate is formed with assistance from a general acid and then hydrolyzed with assistance from a general base. Incubation of recombinant XynB with the newly synthesized active site-directed inhibitor, *N*-bromoacetyl-β-D-xylopyranosylamine, resulted in rapid, time-dependent inactivation of the enzyme ($k_i/K_i = 4.3 \times 10^{-4}$ $s^{-1}mM^{-1}$). Protection from inactivation using xylose or benzyl 1-thio-β-xyloside suggested that the inactivation was active site-directed. Mass spectrometric analysis indicated that incubation of the enzyme with the inactivator resulted in the stoichiometric formation of a new enzyme species bearing the label. Comparative mapping of peptic digests of both the labeled and unlabeled enzyme by HPLC coupled to an electrospray ionization mass spectrometer permitted the identification of a labeled peptide. Sequencing of this peptide by tandem mass spectrometry identified Glu160 within the sequence $_{157}$IWNEPNL$_{164}$ as the site of attachment of the *N*-acetyl-β-D-xylopyranosylamine moiety. Kinetic analysis of the Glu160Ala mutant strongly suggests that this residue is involved in acid/base catalysis as follows. First, a significant difference in the dependence of k_{cat}/K_m on pH as compared to that seen for the wild-type enzyme was found, as expected for a residue that is involved in acid/base catalysis. The changes, however, were not as simple as those seen in other cases. Second, a dramatic decrease (up to 10^5-fold) in the catalytic efficiency (k_{cat}/K_m) of the enzyme with a substrate requiring protonic assistance is observed upon such mutation. In contrast, the catalytic efficiency of the enzyme with substrates bearing a good leaving group, not requiring acid catalysis, is only moderately impaired relative to that of the wild-type enzyme (8-fold). Surprisingly, however, the glycosylation step was rate-limiting for all but the most reactive substrates. Last, the addition of azide as a competitive nucleophile resulted in the formation of a β-xylosyl azide product and increased the k_{cat} and K_m values up to 8-fold while k_{cat}/K_m remained relatively unchanged. Such kinetic behavior is consistent with azide acting competitively with water as a nucleophile in the second step of the enzyme catalyzed reaction involving breakdown of the xylosyl−enzyme intermediate. Together, these results provide strong evidence for a role of Glu160 in acid/base catalysis but suggest that it may be partnered by a second carboxylic acid residue and that the enzyme may function through using acid catalysis involving reverse protonation of active site residues.

The identification of key active site residues in glycosidases is critical for understanding their catalytic mechanisms (*1*), for enzyme classification (*2*), and for bioengineering of glycosyl hydrolases with altered properties (*3*). In the absence of X-ray crystallographic data, many catalytically important residues have been identified through labeling studies using affinity labels or mechanism-based inactivators. Mechanism-based inactivators such as the 5-fluoro-glycosyl fluorides (*4*−*6*) and 2-deoxy-2-fluoro glycosides (*7*−*10*) have proved to be of great utility in reliably labeling the catalytic nucleophile. A reliable method for the labeling of the acid/base catalyst has been elusive, making identification of these residues difficult. A variety of affinity labels that incorporate a sugar moiety to provide specificity for the active site and a reactive group capable of forming stable conjugates with the enzyme have been developed and have met with varying degrees of success. Epoxyalkyl glycosides have proved useful in a number of cases although in some instances they have

† Financial assistance from the Protein Engineering Network of Centres of Excellence of Canada (PENCE) and the Natural Sciences and Engineering Research Council of Canada (NSERC) is gratefully acknowledged. D.J.V. was supported by scholarships from NSERC and the Science Council of British Columbia.

* To whom correspondence should be addressed. Fax (604) 822-8869. E-mail: withers@chem.ubc.ca.

[1] Abbreviations: XynB, *Thermoanaerobacterium saccharolyticum* β-xylosidase; *p*NP, *para*-nitrophenol; *p*NPX, *para*-nitrophenyl β-D-xylopyranoside; *o*NPX, *ortho*-nitrophenyl β-D-xylopyranoside; *m*NPX, *meta*-nitrophenyl β-D-xylopyranoside; 3,4DNPX, 3,4-dinitrophenyl β-D-xylopyranoside; 2,5DNPX, 2,5-dinitrophenyl β-D-xylopyranoside; NBX, *N*-bromoacetyl-β-D-xylopyranosylamine; ISV, ion-source voltage;OR, orifice energy; LC/MS, liquid chromatography MS; MS/MS, tandem MS; ESMS, electrospray MS; TFA, trifluoroacetic acid; TIC, total ion chromatogram; bp, base pairs; kb, kilobases.

10.1021/bi020078n CCC: $22.00
Published on Web 07/09/2002

labeled the catalytic nucleophile (*11*). *N*-Bromoacetylglycosylamines have also met with mixed success. *N*-Bromoacetyl-β-D-galactosylamine labeled a nonessential methionine in the active site of *Escherichia coli* β-galactosidase (*12*), while the gluco analogue was used to label a conserved carboxylate residue in the β-glucosidase from *Manihot esculenta* Crantz (cassava) (*13*). In *Agrobacterium* sp. β-glucosidase inactivation of the enzyme by *N*-bromoacetyl-β-D-glucosylamine was found to follow pseudo-first-order kinetics, but the enzyme was shown by mass spectrometry to be labeled with at least 3 equiv of the reagent (*14*). However, in a study of a xylanase (Cex) from *Cellulomonas fimi*, *N*-bromoacetyl-β-cellobiosylamine was found to label a conserved residue proposed as the acid/base catalyst (*15*). Indeed, later X-ray crystallographic studies on the 2-fluoroglycosyl enzyme (*16*) and kinetic studies of mutants at this position (*17*) provided clear evidence to confirm the identity of the residue so labeled as the acid/base catalytic residue. More recent variations on the *N*-bromoacetylglycosylamines are the α-bromoketone *C*-glycosides, which have been used to label the postulated acid/base catalytic residues of both α- and β-glycosidases (*6*, *18*, *19*).

An alternative method for the identification of the catalytic acid/base residue using a combined mutagenesis and chemical rescue strategy has been developed (*17*, *20*) and proved to be of use in several cases (*19*, *21*, *22*). Studies have shown that for those substrates that bear a very good leaving group that does not require acid catalytic assistance, removal of the acid/base catalytic residue has minimal effect upon the glycosylation step. However, the second step, in which water attacks this intermediate, is significantly compromised when the general base has been deleted since the nucleophilicity of the incoming water molecule is no longer enhanced by base catalysis. Both steps, however, are greatly compromised for substrates with poor leaving groups, requiring acid/base catalysis. Additionally, replacement of the acid/base catalyst in a retaining β-glycosidase with a smaller residue has been proposed to generate a small cavity at the β-face of the substrate adjacent to the anomeric center, and this cavity may accommodate small molecules, particularly anions which may function as competitive nucleophiles. In most cases, increases in the steady-state hydrolysis rate of several 100-fold have been observed when a substrate with a good leaving group, which does not require acid catalysis, is incubated with the enzyme in the presence of a small anion more nucleophilic than water. Such behavior has been shown to result from the interception of the glycosyl−enzyme intermediate by the exogenous nucleophile to yield β-glycosyl adducts of the nucleophile.

This present study describes the synthesis of the novel *N*-bromoacetyl-β-D-xylopyranosylamine (NBX) affinity label and the kinetics of inactivation of the recombinant His_6-tagged xylosidase from *Thermoanaerobacterium saccharolyticum* ($XynBH_6$, see the preceding companion paper for an introduction to this enzyme) upon incubation with this compound. Also, the covalent, stoichiometric labeling of the enzyme and the site of attachment of the label have been determined by comparative mapping of mixtures of labeled and unlabeled peptic digests of the enzyme using ESMS in conjunction with ESMS/MS sequencing of the labeled peptide. We further describe the generation and purification of a mutant of XynB in which the labeled residue, Glu160, is replaced by alanine. Steady-state kinetic analyses of the recombinant XynB and the Glu160Ala mutant with a series of aryl glycosides in the presence and absence of the exogenous nucleophile azide permit assignment of this residue as the catalytic acid/base.

EXPERIMENTAL PROCEDURES

Reagents, Enzymes, and Bacterial Strains. All reagents, enzymes, and bacterial strains were obtained from sources described in the preceding companion paper. Preparation of oligonucleotide primers and DNA sequencing was performed at the Nucleic Acids and Peptide Service facility (NAPS), University of British Columbia.

Site-Directed Mutagenesis by PCR. The gene encoding the His_6-tagged *T. saccharolyticum* β-xylosidase cloned into pET 29b(+) (pET29*xynBH*$_6$), described in the preceding companion paper, was used as a template for mutagenic polymerase chain reaction. A two-primer mutagenic strategy was devised to introduce the desired Glu160Ala mutation and a silent mutation that would introduce a unique *Bgl*II restriction site. The mutagenic primer (forward primer shown below) contained a unique restriction enzyme cleavage site, the silent mutation (in bold below), and the mutation (in bold and italics). The reverse primer (shown below) contained a unique restriction enzyme cleavage site. The forward primer was as follows:

5'-GTC TTG AAG TGG CAA TTT G**AG ATC** TGG AAT GC***A*** CCA AAC TTA AAA GAG-3'
*Msc*I *Bgl*II

The reverse primer was as follows:

5'-ATC TCT TTC TTC GAA AAC GTC GCT GCT-3'
*BstB*1

A mixture containing plasmid pET29*xynBH*$_6$ as a template and the two primers just described was heated to 95 °C, after which the PCR reaction was started by adding 5 units of *Pwo* DNA polymerase (Boehringer Mannheim). Thirty PCR cycles (45 s at 94 °C, 45 s at 56 °C, and 70 s at 72 °C) were performed in a thermal cycler (Perkin-Elmer, GeneAmp PCR System2400). Following agarose gel electrophoresis of the PCR reaction, the sole product, an approximately 500 bp dsDNA fragment, was isolated using the Qiaquick PCR purification kit according to the manufacturer's protocol (Qiagen). The restriction endonucleases *Msc*I and *BstB*1 were used in separate digests to generate a double sticky end fragment that was purified using the Qiaquick PCR purification kit. To prepare nondcm methylated plasmid DNA, pET29x*ynBH*$_6$ was transformed into electrocompetent JM110 cells and selected by the kanamycin resistance conferred by the plasmid. Single colonies were selected and grown overnight in LB_{kan}, and DNA was isolated via the mini-preparation technique. This nondcm methylated DNA was digested sequentially with *Msc*I and *BstB*I endonucleases and purified in the same manner as described. Ligation of the digested gel purified pET29*xynBH*$_6$ and the digested PCR fragment was accomplished using T4 DNA ligase (1 unit/10 ng DNA) at a ratio of 10:1 (insert to vector) at 25 °C. The cloned product, called pET29x*ynBH*$_6$*(E160A)*, was subsequently transformed into electrocompetent Topp10 cells, selected by the kanamycin resistance conferred by pET-

29b(+). Single colonies were selected and grown overnight in LB_{kan}, and DNA was isolated via the minipreparation technique. Restriction endonuclease digest using *Bgl*II revealed positive clones. Topp10 transformed cells were used for preparation of large amounts of plasmid pET29*xynBH*$_6$ (Qiagen Plasmid Maxi kit) and long-term storage of the vector as glycerol stock.

Overexpression and Purification of His$_6$*-Tagged XynB-(E160A).* An identical protocol to that used in the preceding companion paper for the purification of the $XynBH_6$ enzyme was used for the preparation of the mutant $XynBH_6$(E160A) enzyme except that in the initial step the plasmid pET29-*xynBH*$_6$*(E160A)* was used to transform the electrocompetent BL21(DE3) cells. Care was taken during the purification of $XynBH_6$ and $XynBH_6$(E160A) to avoid wild-type contamination of the mutant enzyme. The purification of the $XynBH_6$(E160A) was conducted with equipment that had never come in contact with any $XynBH_6$. The $XynBH_6$-(E160A) mutant enzyme was concentrated to ~5 mg/mL using a Centriprep concentrator (30 kDa cutoff) from Amicon and dialyzed using a Slide-A-Lyzer (10 kDa cutoff) from Pierce against 50 mM phosphate buffer pH 7.00.

General Procedures and Synthesis. All buffer chemicals and other reagents were obtained from the Sigma/Aldrich Chemical Co. unless otherwise noted. Synthetic reactions were monitored by TLC using Merck Kieselgel 60 F_{254} aluminum-backed sheets. Compounds were detected by charring with 10% ammonium molybdate in 2 M H_2SO_4 and heating. ^{1}H NMR spectra were recorded on a Bruker WH-400 spectrometer at 400 MHz (chemical shifts are quoted relative to TMS ($\delta = 0.00$) as an internal standard).

N-Bromoacetyl-β-D-Xylopyranosylamine (NBX). Bromoacetic anhydride (*23*) (121 mg, 2.15 mmol) was added to a solution of β-D-xylosylamine (*24*) (152 mg, 1.02 mmol) in DMF (1.5 mL) over 15 min. The mixture was stirred for 1 h at room temperature, poured into ice-cold anhydrous ether and stirred for 1 h. The ether was decanted and the residual gum crystallized from MeOH to yield the desired product as fine white needles (61 mg, 22%). mp 150−151 °C. ^{1}H NMR (400 MHz, CD_3OD) δ: 4.81 (1 H, d, $J_{1,2} = 8.8$ Hz, H-1), 3.87 (2 H, CH_2Br), 3.83 (1 H, dd, $J_{5,4} = 5.2$ Hz, $J_{5,5'} = 11.2$ Hz, H-5), 3.47 (1 H, ddd, $J_{4,3} = 8.8$ Hz, $J_{4,5'} = 10.3$ Hz, H-4), 3.35 (1 H, dd, $J_{3,2} = 8.8$ Hz, H-3), 3.26 (1 H, dd, H-5′), 3.25 (1 H, dd, H-2). Anal. Calcd for $C_7H_{12}BrNO_5$: C, 31.13; H, 4.48; N, 5.19. Found: C, 31.52; H, 4.40; N, 5.12.

Labeling and Proteolysis of T. saccharolyticum β-Xylosidase. Labeling of *T. saccharolyticum* β-xylosidase (1.3 mg/mL) was accomplished by incubating the enzyme with NBX (6.0 mM) for 20 min at 30 °C in 50 mM sodium citrate, pH 5.50, in a total volume of 30 μL. This sample was then analyzed immediately by injecting the mixture onto a reverse-phase column (PLRP-S, 1 × 50 mm) equilibrated with solvent A [solvent A: 0.05% trifluoroacetic acid (TFA)/2% acetonitrile in water] on an Ultrafast Microprotein Analyzer (Michrom BioResources Inc., Pleasanton, CA). Elution of the enzyme directly into the mass spectrometer was accomplished using solvent A at a flow rate of 50 μL/min.

Proteolytic digestion of the enzyme was performed by mixing the labeled enzyme (30 μL of 1.3 mg/mL) with 4 μL of 2.1 M sodium phosphate pH 1.7, and 4 μL of 1 mg/mL pepsin in 200 mM sodium phosphate, pH 2.0. This sample and a control in which the enzyme was not exposed to the inhibitor were incubated at 25 °C for 30 min. After this time, the sample was frozen at −78 °C. Analysis of these samples by ESMS revealed that the digest time chosen ensured complete digestion of the enzyme and generated peptides of a size suitable for sequencing by MS/MS.

ESMS Analysis of the Proteolytic Digest. Mass spectra were recorded on a PE-Sciex API 300 triple-quadrupole mass spectrometer (Sciex, Thornhill, Ontario, Canada) equipped with an Ionspray ion source. Peptides were separated by reverse-phase HPLC on an Ultrafast Microprotein Analyzer (Michrom BioResources Inc., Pleasanton, CA) directly interfaced with the mass spectrometer. In each of the MS experiments, the proteolytic digest was loaded onto a C-18 column (Reliasil, 1 × 150 mm) equilibrated with solvent A [solvent A: 0.05% trifluoroacetic acid (TFA)/2% acetonitrile in water]. Elution of the peptides was accomplished using a gradient (0−60%) of solvent B over 60 min followed by 100% solvent B over 2 min (solvent B: 0.045% TFA/80% acetonitrile in water). Solvents were pumped at a constant flow rate of 50 μL/min. Spectra were obtained in the single-quadrupole scan mode (LC/MS) or the tandem MS product-ion scan mode (MS/MS). In the single-quadrupole mode (LC/MS), the quadrupole mass analyzer was scanned over a mass-to-charge ratio (m/z) range of 300−2200 Da with a step size of 0.5 Da and a dwell time of 1.5 ms per step. The ion source voltage (ISV) was set at 5.5 kV, and the orifice energy (OR) was 45 V. In the tandem MS daughter-ion scan mode, the spectra were obtained in separate experiments by selectively introducing the labeled ($m/z = 1075$) or unlabeled ($m/z = 885$) parent ion from the first quadrupole (Q1) into the collision cell (Q2) and observing the product ions in the third quadrupole (Q3). Thus, Q1 was locked on either m/z 1075 or m/z 885; the Q3 scan range was 50−1100; the step size was 0.5; the dwell time was 1 ms; ISV was 5 kV; OR was 45 V; Q0 = −10; IQ2 = −48.

Enzyme Kinetics. Michaelis−Menten parameters for aryl xylosides were determined by continuous measurement of the release of the substituted phenol product using a Pye-Unicam PU8700 as described previously (*25*, *26*). Reactions were monitored at appropriate wavelengths using the same extinction coefficients reported in the preceding paper. Phenol pK_a values used were those reported in Kempton and Withers (*25*). Unless indicated otherwise, reaction mixtures, in 25 mM citrate/25 mM phosphate buffer (pH 5.5 for $XynBH_6$ and pH 6.5 for $XynBH_6$(E160A)) containing 0.1% BSA (buffer A) at 37 °C, were preincubated in the cell-holder at the appropriate temperature for 10 min prior to addition of enzyme. Sodium azide was included in mixtures as indicated, and care was taken to ensure that the desired pH of the assay mixture was obtained. Enzyme-catalyzed hydrolysis for each substrate was measured at 8−10 different substrate concentrations ranging from about 0.14K_m to 7K_m, where practical. Values for K_m and k_{cat} were determined from the initial rates of hydrolysis (V_o) versus substrate concentration, by nonlinear regression analysis using the computer program GraFit 3.0 (*27*).

The inactivation of β-xylosidase by NBX was monitored by incubation of the enzyme (0.61 mg/mL) in buffer A at 37 °C in the presence of various concentrations of the inactivator (1.5−17.9 mM). Residual enzyme activity was determined at several time intervals by addition of an aliquot

($5\ \mu$L) of the inactivation mixture to a solution of *p*NPX ($135\ \mu$M, $800\ \mu$L) in buffer A. Pseudo-first-order rate constants at each inactivator concentration (k_{obs}) were determined by fitting each inactivation curve to a first-order rate equation. The second-order rate constant for the inactivation process was determined by fitting each k_{obs} value to the equation

$$k_{obs} = [E]_o(k_i/K_i)$$

The active-site-directed nature of the inactivation was proven by demonstrating protection against inactivation by a competitive inhibitor. Inactivation mixtures ($40\ \mu$L) containing 0.61 mg/mL enzyme and 11.9 mM NBX were incubated in the absence and presence of either benzyl β-D-thioxylopyranoside (10.6 mM, $K_i = 5.3$ mM) or xylose (80.8 mM, $K_i = 20$ mM). At various time intervals, aliquots ($5\ \mu$L) were removed and assayed for residual activity as described above.

pH Dependence of k_{cat}/K_m. The k_{cat}/K_m values for the hydrolysis of chromogenic phenyl xylosides at each pH were determined from progress curves at low substrate concentrations as follows. For the $XynBH_6$(E160A) mutant, a solution of 3,4DNPX ($2.4\ \mu$M, $0.01-0.2 \times K_m$), 0.1% BSA, and the appropriate buffer was warmed to 37 °C. The reactions were initiated by the addition of a $10\ \mu$L aliquot of enzyme (0.4−5 mg/mL), and the release of phenolate was monitored at 400 nm (3,4DNPX) for 5−10 min, at which time it was apparent that 5−7 half-lives had passed. The pH of the reaction mixture was then checked to ensure that no significant change in pH had occurred during the course of the assay. The change in absorbance with time was fitted to a first-order rate equation using the program GraFit 3.0 (*27*), yielding values for the pseudo-first-order rate constant (k_{obs}) at each pH value. Since at low substrate concentrations ($[S] \ll K_m$) the reaction rates are given by the equation

$$v = k_{cat}[E]_o[S]/K_m$$

the k_{obs} values correspond to $[E]_o k_{cat}/K_m$. Thus, k_{cat}/K_m values can be extracted by division of these obtained rate constants by the enzyme concentration. The buffers used each contained 0.1% BSA (w/v) and were as follows: pH 4.5−6.5, 50 mM citrate and 150 mM sodium chloride; pH 6.5−8.0, 50 mM phosphate and 150 mM sodium chloride; pH 8.0−9.5, 50 mM AMPSO and 150 mM sodium chloride. By analyzing the bell-shaped k_{cat}/K_m versus pH plots using GraFit 3.0, we assigned two apparent pK_a values of ionizable groups. The stability of the enzyme was examined over the pH range and assay time of the study by adding enzyme at the same concentration as examined in the pH study to a preincubated cell containing 0.1% BSA and the appropriate buffer at 37 °C. After 10 min, 1 aliquot of the mixture was removed and injected into another preincubated solution of 3,4DNPX ($600\ \mu$M), 25 mM citrate/25 mM phosphate buffer pH 6.5. Data were retained for those pH values at which the enzyme was stable during the assay period. Data were discarded if more than 10% enzyme death occurred over a 10 min period.

Analysis of the Products of Enzymatic Hydrolysis. Mixtures containing 5 mM 3,4DNPX, 2 M azide, and 0.5 mg/mL of $XynBH_6$(E160A) or 0.1 mg/mL of $XynBH_6$ in 50 mM phosphate buffer (pH 7.5) were incubated at 37 °C overnight. One aliquot of the reaction mixtures and a standard of

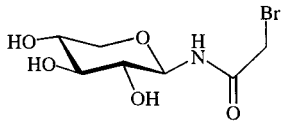

FIGURE 1: Chemical structure of the affinity label *N*-bromoacetyl-β-xylopyranosylamine.

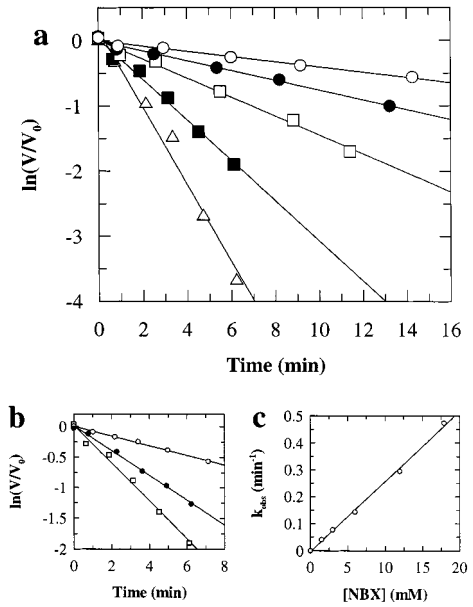

FIGURE 2: Inactivation of *T. Saccharolyticum* β-xylosidase by NBX. (a) Semilogarithmic plot of residual enzyme activity vs time at the indicated inactivator concentration: (○) 1.49, (●) 2.99, (□) 5.97, (■) 11.94, and (△) 17.91 mM. (b) Inactivation with 11.9 mM alone (○) and in the presence of 80.8 mM xylose (□) or 10.6 mM BTX (●). (c) Plot of the first-order rate constants from panel a.

β-xylosyl azide were applied to a 0.2 mm silica gel aluminum TLC plate (#60 F_{254}; E. Merck) and allowed to air-dry. The developing solvent was a mixture of ethyl acetate/methanol/water (7:2:1 v/v/v). After development, the chromatograms were air-dried for 5 min, then dipped in a solution of 10% H_2SO_4 in methanol, and heated until the charred reaction products were visible.

^{1}H NMR Spectrometry of the Products of Enzymatic Hydrolysis. Mixtures containing 5 mM 3,4DNPX, 2 M azide, and 0.5 mg/mL of $XynBH_6$(E160A) or 0.1 mg/mL of $XynBH_6$ in 50 mM phosphate buffer (pH 7.5) were incubated at 37 °C overnight. Enzyme was removed by passing the solution through a 10 kDa cutoff polysulfone membrane (ultrafree-MC; Millipore). Samples of the filtrate were prepared for ^{1}H NMR analysis by repeated freeze-drying and dissolving in DMSO-D_6. Spectra were recorded with a Bruker 400 MHz spectrometer and compared against a standard of β-xylosyl azide (*28*).

RESULTS

Inactivation of the Enzyme. Incubation of *Thermoanaerobacterium saccharolyticum* β-xylosidase with NBX (Figure 1) resulted in pseudo-first-order inactivation of the enzyme in a rapid, time-dependent manner (Figure 2a). The enzyme inactivation rate with NBX was shown to be dependent on the concentration of inactivator although saturation was not observed (Figure 2c). Analysis of the data as described in the methods and materials section permitted the calculation of the second-order rate constant for the inactivation process

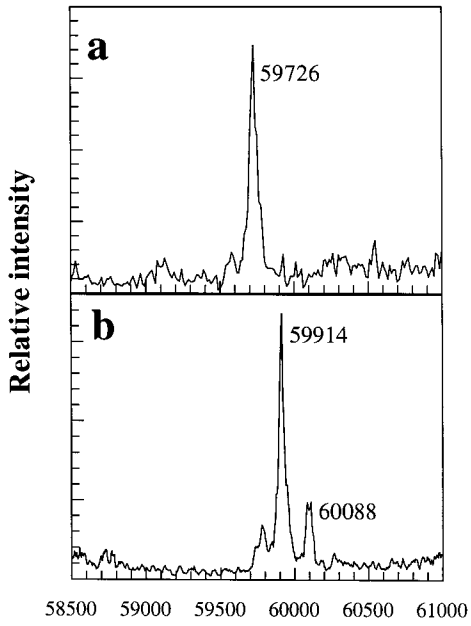

FIGURE 3: Transform of the electrospray mass spectrum of (a) native $XynBH_6$ and (b) $XynBH_6$ after incubation with 21 mM NBX for 30 min.

($k_i/K_i = 4.3 \times 10^{-4}$ $s^{-1}mM^{-1}$) with NBX (11.9 mM). Incubation of the enzyme with NBX in the presence of the competitive inhibitors xylose (80.8 mM, $K_i = 20$ mM) or benzyl 1-thio-β-D-xylopyranoside (BTX, 10.6 mM, $K_i = 5.3$ mM) resulted in lower apparent inactivation rate constants. In the absence of xylose or BTX, the apparent inactivation rate constant was 0.0048 s^{-1}, while in the presence of xylose and BTX, this dropped to 0.0013 and 0.0032 s^{-1}, respectively (Figure 2b).

Stoichiometry of Incorporation of Inactivator Studied by ESMS. The mass of the native $XynBH_6$ was found by ESMS to be 59726 ± 6 Da (Figure 3a). After inactivation of the enzyme with NBX, a new species was observed with a mass of 59914 ± 6 Da (Figure 3b). The difference (188 Da) corresponds to the incorporation of a single *N*-acetyl-β-xylosamine moiety (190 Da). A second minor peak at 60 088 Da presumably corresponds to a very small amount of doubly labeled enzyme.

Identification of the Labeled Active Site Peptide by ESMS. Peptic hydrolysis of the *N*-acetylxylosylamine−enzyme resulted in a mixture of peptides that were separated by reverse-phase HPLC using the ESMS as a detector. A sample of unlabeled enzyme was also subjected to peptic digestion. When these two mixtures were analyzed in separate experiments by scanning in the normal LC/MS mode, the total ion chromatogram in both cases showed a large number of peaks, each corresponding to one or more peptides in the digest mixture (Figure 4a,b). The peptide bearing the *N*-acetyl-β-xylosylamine label was then located by careful comparison of the TIC's of the labeled and unlabeled enzyme digests. It was expected that the masses of the relevant labeled and unlabeled active site peptides would differ by the mass of the *N*-acetyl-β-xylosylamine label (190 Da). The masses of peptides corresponding to peaks found solely in one of the TIC's from either the labeled or unlabeled enzyme were therefore compared. In this way, a peptide with a mass of 1075 ± 1 Da was found only in the TIC of the labeled enzyme digest at 29.3 min, and this peptide was therefore a

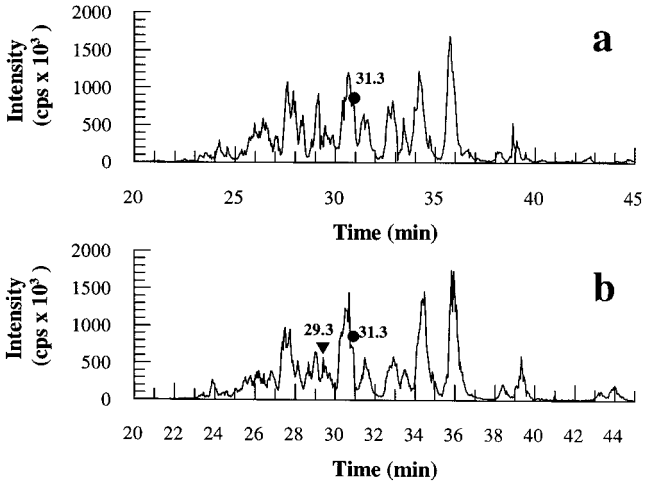

FIGURE 4: ESMS experiments on peptic digests of $XynBH_6$. (a) TIC of the unlabeled enzyme indicating the position of the unlabeled peptide of *m*/*z* 885 (●). (b) TIC of the enzyme labeled with NBX where ▼ indicates the position of the newly observed peak corresponding to the labeled peptide *m*/*z* 1075 and ● indicates the position of the unlabeled peptide of *m*/*z* 885.

good candidate for the active site peptide of interest. A search of the TIC of the unlabeled enzyme digest for a possible unlabeled peptide of mass 885 ± 1 Da, corresponding to the mass difference between the peptide of mass 1075 Da and the mass of the *N*-acetylxylosylamine label (190 Da), yielded a peak at 31.3 min (Figure 4b). The TIC of the labeled enzyme digest was examined for the same peptide, and a peak was found at the same position, but at a much lower intensity. These results suggest that the peptide of mass 1075 Da is likely the modified peptide and that the appearance of the peptide of 885 Da in the labeled sample was likely due to incomplete inactivation of the enzyme and/or cleavage of the *N*-acetylxylosylamine label during proteolysis or chromatography. (Both the labeled and unlabeled peptides were purified by HPLC-MS using the same conditions outlined above, except that a flow splitter was used to divert 90% of each sample away from the mass spectrometer. 500 μL fractions were collected.)

Peptide Sequencing. Information on the sequence of the peptide bearing the label and its site of attachment was obtained in separate experiments by fragmentation of the two peptides of interest (*m*/*z* 1075 and *m*/*z* 885) in the daughter ion scan mode. The parent ions in both the labeled peptide (Figure 5a) and the unlabeled peptide (Figure 5b) appear as singly charged species. Peaks resulting from B ions of the unlabeled peptide correspond to IW (*m*/*z* 300), IWN (*m*/*z* 414), IWNE (*m*/*z* 543), IWNEP (*m*/*z* 640), and IWNEPN (*m*/*z* 754). Peaks arising from Y″ ions of the unlabeled peptide correspond to NL (*m*/*z* 246), PNL (*m*/*z* 343), EPNL (*m*/*z* 472), NEPNL (*m*/*z* 586), and WNEPNL (*m*/*z* 772). This information, in conjunction with the mass of the intact peptide and the primary sequence of the enzyme, clearly defines the unlabeled peptide as $_{158}$IWNEPNL$_{164}$. In a separate MS/MS sequencing experiment, the purified, labeled peptide was also subjected to fragmentation. The peaks arising from B ions of the labeled peptide (Figure 5a where * denotes the label) include IW (*m*/*z* 300), IWN (*m*/*z* 414), IWNE* (*m*/*z* 733), and IWNE*PN (*m*/*z* 942). Peaks arising from Y″ ions of the labeled peptide correspond to NL (*m*/*z* 246), PNL (*m*/*z* 343), E*PNL (*m*/*z* 662), and NE*PNL (*m*/*z*

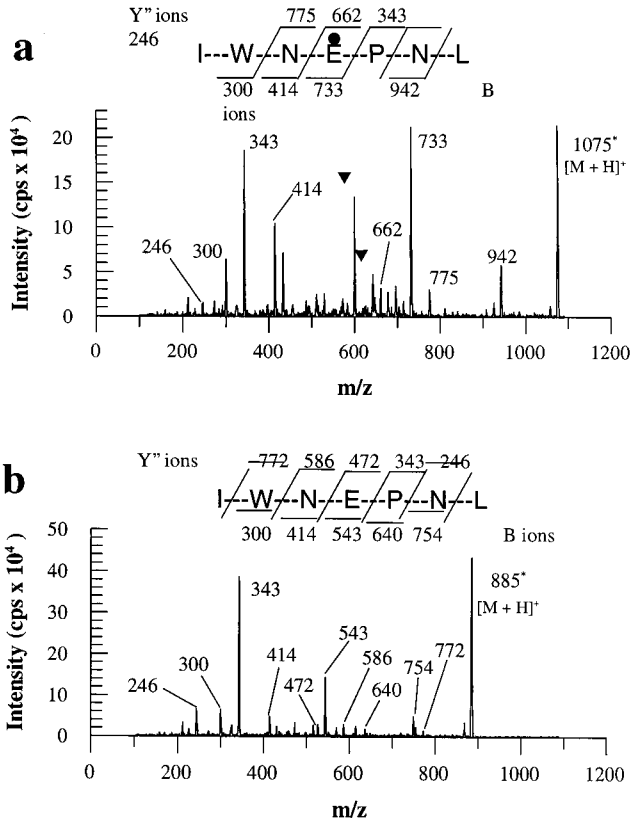

FIGURE 5: ESMS/MS daughter-ion spectra of the (a) labeled peptide (*m*/*z* 1075, in the singly charged state) and the (b) unlabeled peptide (*m*/*z* 885, in the singly charged state). Observed Y″ and B series fragments are shown above and below the peptide sequences repectively. (●) The site of attachment of the label.

775). Additional peaks arising from the fragmentation of the ester bond linking the label and peptide are marked by (▼) in Figure 5a.

Production and Purification of the Enzymes. The *xynB* gene was mutated to code for the enzyme bearing a *C*-terminal His_6-tag ($XynBH_6$) and cloned into the high expression vector pET29b(+). The mutant $XynBH_6$(E160A) was prepared from the pET29b(+)*xynBH*$_6$ construct, and complete sequencing of both genes confirmed the desired DNA sequence. High-yielding expression of the enzymes from this expression system was obtained as revealed by SDS−PAGE analysis of a sample of the cell extract and pure enzyme (data not shown). During the purification of the enzymes, great care was taken to eliminate the possibility of contamination of $XynBH_6$(E160A) by $XynBH_6$. Purification of the enzymes using metal chelate chromatography provided a rapid route to the purified enzymes which, by SDS−PAGE analysis, migrated as a single band (>95% by inspection), at the same position as that of a sample of the recombinant XynB. The recombinant $XynBH_6$ enzyme exhibited kinetic parameters for the hydrolysis of *p*NPX (K_m = 36 μM, k_{cat} = 4.6 s^{-1}) very similar to those of the recombinant XynB enzyme obtained in a previous study (K_m = 26 μM, k_{cat} = 4.0 s^{-1}) (*29*). These data indicate that the polyhistidine tag does not have any deleterious effect on the enzyme activity.

pH Profiles. Values of k_{cat}/K_m were determined for the hydrolysis of *p*NPX by $XynBH_6$ and 3,4DNPX by $XynBH_6$-(E160A) as a function of pH within the pH stability range (4.5−9.5) of the recombinant enzyme. The mutation had a

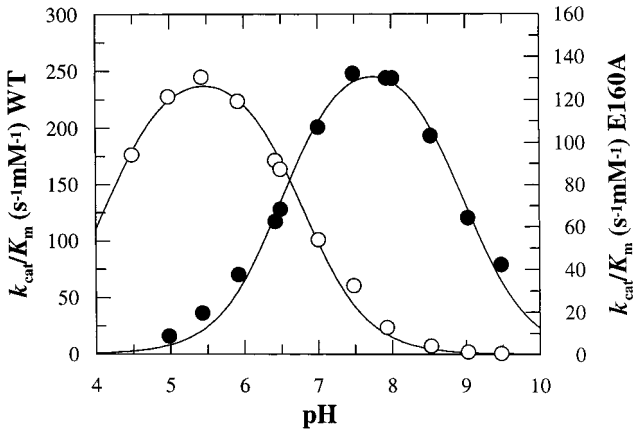

FIGURE 6: pH dependence of k_{cat}/K_m for the wild-type $XynBH_6$ xylosidase (○) and $XynBH_6$(E160A) xylosidase (●). The lines shown represent fits to the data for enzymes with two ionizable residues.

significant effect on the pH profile of the enzyme as shown in Figure 6. Fitting the data to a double titration curve yielded the following pK_a values: for $XynBH_6$, pK_{a1} = 4.1 ± 0.1 and pK_{a2} = 6.8 ± 0.1; for $XynBH_6$(E160A), pK_{a1} = 6.5 ± 0.1 and pK_{a2} = 9.0 ± 0.1.

Substrate Reactivity of XynBH$_6$ *and XynBH*$_6$*(E160A).* The Michaelis−Menten kinetic parameters for the hydrolysis of 2,5DNPX, 3,4DNPX, *p*NPX, *o*NPX, and *m*NPX by both $XynBH_6$(E160A) and $XynBH_6$ were determined (Table 1). The mutation of the labeled glutamic acid residue to an alanine results in an enzyme with impaired, yet significant, catalytic activity. Brønsted plots of log(k_{cat}/K_m) against pK_a of the aryl leaving group for both enzymes provide good correlations with β_{lg} = −0.31 for $XynBH_6$ and β_{lg} = −1.4 for $XynBH_6$(E160A) (n = 5, r = −0.98, Figure 7a). The Brønsted plot of log(k_{cat}) for the hydrolysis of a series of aryl xylosides by the wild-type enzyme against pK_a of the leaving group reveals no dependence on leaving group ability in the pK_a range of 5−8 (Figure 7b). The Glu160Ala mutant, however, shows a strong dependence on leaving group ability (β_{lg} = −0.65, n = 5, r = −0.96).

Product Analysis. Thin-layer chromatographic analysis of reaction mixtures containing 3,4DNPX and 2000 mM azide and either $XynBH_6$ or $XynBH_6$(E160A) revealed the formation of a product distinct from xylose and 3,4DNP but identical in mobility to a standard of β-D-xylosyl azide prepared by chemical synthesis (*28*). Additionally, analysis of a mixture of the products from both reactions by ^{1}H NMR revealed signals diagnostic of β-D-xylosyl azide (^{1}H NMR (400 MHz, DMSO-D_6) δ: 4.42 (1 H, d, $J_{1,2}$ = 8.5 Hz, H-1), 3.75 (1 H, dd, $J_{5eq,5ax}$ = 11.1 Hz, $J_{5eq,4}$ = 5.2 Hz, H-5_{eq})). The other signals were obscured by signals arising from solvent, buffer, and other products.

Effect of Competitive Nucleophiles on Rates of Hydrolysis by XynBH$_6$*(E160A).* The rates of cleavage of a fixed concentration of 3,4DNPX by both the $XynBH_6$(E160A) and $XynBH_6$ were determined in the presence of varying concentrations (0−2000 mM) of sodium azide (Figure 8). The effects of other nucleophiles, including formate, acetate, and fluoride, were also investigated in the hope that greater rate increases could be observed. These alternative anionic nucleophiles, however, were found to give rise to much smaller rate accelerations as compared to azide (Data not

Table 1: Kinetic Parameters for the Hydrolysis of Aryl Xylosides by $XynBH_6$ Carried out at pH 5.5 and $XynBH_6$(E160A) Carried out at pH 6.5

substrate	pK_a	enzyme	k_{cat} (s^{-1})	ratio k_{cat} [Wt/E160A]	K_m (μM)	k_{cat}/K_m (s^{-1} mM^{-1})	ratio (k_{cat}/K_m) [Wt/E160A]
2,5DNPX	5.15	Wild-type	7.3	8.7	11	670	7.9
		E160A	0.84		10	84	
3,4DNPX	5.36	Wild-type	8.9	11	10	900	16
		E160A	0.78		14	56	
*p*NPX	7.18	Wild-type	9.7	2.4×10^2	36	270	9.4×10^2
		E160A	4.0×10^{-2}		1.4×10^2	0.28	
*o*NPX	7.22	Wild-type	9.9	110	46	220	1.9×10^2
		E160A	9.0×10^{-2}		80	1.1	
*m*NPX	8.39	Wild-type	11	2.1×10^3	150	73	7.0×10^4
		E160A	5.2×10^{-3}		4.9×10^3	1.1×10^{-3}	

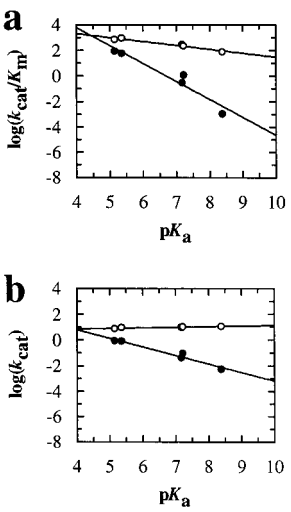

FIGURE 7: Brønsted relationships for $XynBH_6$ (○) and $XynBH_6$-(E160A) (●). The data for the (a) log(k_{cat}/K_m) and (b) log(k_{cat}) were taken from Table 1.

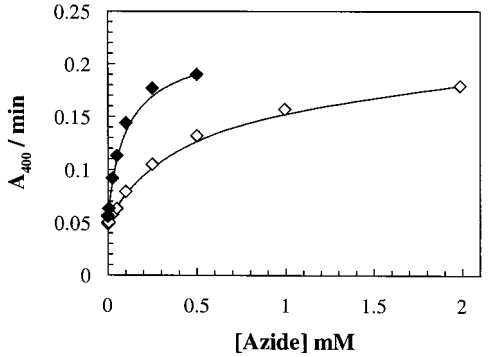

FIGURE 8: Comparison of the effect of azide on the rate of hydrolysis of 3,4DNPX (49 μM) by (◇) 2.3 μg/mL $XynBH_6$ and (◆) 31.2 μg/mL $XynBH_6$(E160A).

shown). Consequently, azide was chosen as the nucleophile to be used for all the detailed chemical rescue studies. Additional experiments using a range of sodium chloride concentrations revealed that there was little effect on the rate of 3,4DNPX hydrolysis by $XynBH_6$ arising from ionic strength. Indeed, 2 M sodium chloride resulted only in a 20% decrease in k_{cat}. The superiority of azide as an exogenous nucleophile in chemical rescue studies of glycosidases has been demonstrated in several previous cases (*20, 30*).

Having decided on the use of azide for the chemical rescue studies, we carried out a more detailed analysis of the effect of azide on the $XynBH_6$(E160A) mutant enzyme. The rates of cleavage of a range of concentrations of 3,4DNPX

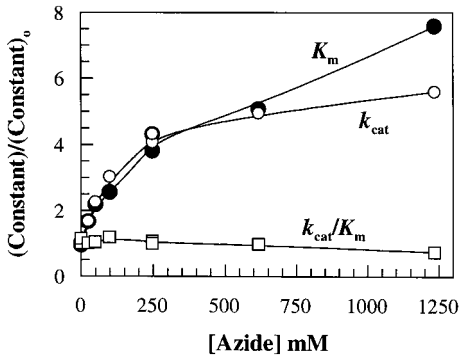

FIGURE 9: Effect of azide on the kinetic parameters for the hydrolysis of 3,4DNPX by $XynBH_6$(E160A).

(typically $0.3-5 \times K_m$) by $XynBH_6$(E160A) were determined in the presence of varying concentrations (0−2000 mM) of sodium azide. Both k_{cat} and K_m increased as a function of azide concentration (Figure 9), leveling off at higher concentrations. In marked contrast, k_{cat}/K_m remained essentially unchanged or even slightly decreased across the range of azide concentrations studied.

DISCUSSION

Inactivation of $XynBH_6$ and Identification of the Labeled Residue. Despite the absence of saturation kinetics that might suggest a specific site-directed inactivation of the enzyme, the relatively rapid inactivation of $XynBH_6$ in the presence of NBX suggests that this process may be specific for a particular site on the enzyme. Indeed, the observed protection from inactivation in the presence of xylose or BTX indicates that NBX and xylose or BTX are competing for the same site, suggesting that the inactivation does occur at the enzyme active site. Additionally, the mass difference between inactivated and native $XynBH_6$ is 188 Da and corresponds, within error, to the addition of a single *N*-acetyl-β-xylosylamine label (190 Da).

Comparative mapping of the digests of the unlabeled and NBX-labeled enzyme allows the tentative identification of two peptides, one having a mass of 1075 Da as the modified peptide bearing the label and the other having a mass of 885 Da as the same peptide but not bearing the label. Tandem mass spectrometric sequencing of these two peptides confirms this assignment and clearly permits identification of the active site peptide bearing the label as $_{157}$IWNEPNL$_{164}$ within which the site of attachment is Glu160. The identification of this residue, the sole carboxyl residue within the peptide, is encouraging. In all cases to date where the identity of the acid/base catalytic residue in a glycoside hydrolase

```
xynb-thesa      137 VVSHFIERYGIEEVRTWLFEVWNEPNLVNFWKDANKQEYFKLYEVT 182
xynd_calsa       93 VVKHFIDRYGEKEVVQWPFEIWNEPNLNVFWKDANQAEYFKLYEVT 138
xynB_calsa      140 LARHLISRYGKNEVREWFFEVWNEPNLKDFFWAGTMEEYFKLYKYA 185
idua_human      159 LARRYIGRYGLAHVSKWNFETWNEPDHHDFDNVSMTMQGFLNYYDA 204
idua_canfa      158 LARRYIGRYGLSYVSKWNFETWNEPDHHDFDNVTMTLQGFLNYYDA 203
idua_mouse      149 LARRYIGRYGLTHVSKWNFETWNEPDHHDFDNVSMTTQGFLNYYDA 194
CONSENSUS           :  : * ***   *  * ** **●*:   *       : *  *  :
```

FIGURE 10: Partial multiple sequence alignment of the enzymes comprising family 39 of glycosyl hydrolases. The consensus sequence is shown at the bottom of the alignment, with (*) indicating fully conserved amino acid residues and (:) indicating similar residues. Numbers to the left denote residue positions. The abbreviations used, references to the published sequence, and data bank accession numbers are as follows: xynb-thesa, β-xylosidase from *T. saccharolyticum* (*39*, SwissProt identifier P36906); xynb-calsa, β-xylosidase from *Caldocellum saccharolyticum* (*40*, SwissProt identifier P23552); idua-human, α-iduronidase from *Homo sapiens* (*41*, SwissProt identifier P35475); idua-mouse, α-iduronidase from *Mus musculus* (*42*, SwissProt identifier P48441); idua-canfa, α-iduronidase from *Canis familiaris* (*43*, SwissProt identifier Q01634). The acid/base catalytic residue identified in this work, E160A in XynB, is indicated by ●.

has been determined, it has been found to be either an Asp or Glu side chain.

Sequence Conservation and Alignment. Multiple sequence alignments of the members of family 39 glycosyl hydrolases revealed sequence similarities between the xylosidases and iduronidases of this family to be less than 16%. This overall sequence similarity is primarily accounted for by a few discrete regions that demonstrate significant sequence similarity across all family members, such as the segment approximately 100 residues before the catalytic nucleophile, which contains the glutamic acid that has been labeled and mutated within this study. This residue is completely conserved throughout all members of family 39 of glycoside hydrolases and is contained within the short conserved sequence $_{159}$NEP$_{161}$ (Figure 10). This sequence is reminiscent of the NEP sequence within which the acid/base catalytic residue is found approximately 100 residues before the catalytic nucleophile in several other β-glycosidases, including the family 1 *Agrobacterium* sp. β-glucosidase, the family 2 *Escherichia coli* β-galactosidase, and the family 10 xylanases. These enzyme classes, along with enzyme families 5, 17, 26, 30, 35, 39, 42, and 53, have been assigned as members of clan GH-A, a superfamily of glycosyl hydrolases with an α/β barrel fold (*31*). The results of the kinetic analysis of XynBH$_6$ and XynBH$_6$(E160A) and the complete conservation of this residue across all members of this family provide very strong evidence that Glu160 is indeed an acid/base catalyst, as suggested previously on the basis of predictions (*31*) and by studies on the family 39 β-xylosidases from *Bacillus stearothermophilus* (*19*).

Kinetic Analysis of the Mutant Enzyme. Since both the sequence predictions and the labeling study point to E160 as the acid/base catalytic residue, a detailed analysis of a mutant enzyme modified at this position was carried out to confirm the assignment and provide insights into how acid/base catalysis is effected. Significant differences should be observed in the pH dependence of the activity of the mutant enzyme relative to that of the wild-type. Bell-shaped pH profiles are commonly seen when plotting k_{cat}/K_m versus pH values for wild-type glycosidases and usually reflect the ionizations of the catalytic nucleophile and the acid/base residue of the free enzyme (*32*). The approximate 2 pH unit shift of the bell-shaped k_{cat}/K_m pH profile to higher pH upon removal of the acid/base residue is unexpected and is markedly different from that seen in the study on the *Bacillus stearothemophilus* β-xylosidase. Elimination of the acid/base residue in several other retaining β-glycosidases, including the *B. stearothermophilus* β-xylosidase (*19*), has simply resulted in the elimination of the basic limb of the pH profile corresponding to pK_{a2}, accompanied by a substantial decrease in activity (*17*, *22*). It is interesting to speculate that in XynBH$_6$ a third ionizable group in the active sites having a pK_a value greater than 6.8 is required for efficient catalysis. This ionization would be masked in XynBH$_6$ by the ionization of the acid/base catalyst. Thus, only on removal of the acid/base catalyst residue, as in XynBH$_6$(E160A), would the ionization of this third residue become apparent. Another alternative explanation may be that the shift is a consequence of reverse protonation (*33*) within the wild-type enzyme, as seen recently for the "acidic" family 11 xylanases (*34*, *35*). In that case the acid/base residue is in fact one of a pair of carboxylic acids that function together to deliver a proton. Upon formation of the glycosyl−enzyme intermediate, a very strong hydrogen bond is formed between the two carboxyl groups. This interaction serves to stabilize the intermediate and, more importantly, the flanking transition states, thereby accelerating the first (glycosylation) step. An interesting consequence of this mechanism is that the pK_a of one of the acid/base "group" is lower than the pK_a of the nucleophile, thus only a small fraction of the enzyme is in the "correct" ionization state for catalysis. Nonetheless, the rate acceleration provided by the strong hydrogen bond is sufficient to overcome this disadvantage, giving an enzyme with good activity (Figure 11).

We therefore suggest that the true microscopic pK_a of the nucleophile may be quite high and the pK_a of the acid/base residue may be much lower than appears to be the case (reverse protonation). Upon deletion of the carboxyl group of the acid/base catalytic residue, the true microscopic pK_a of the nucleophile residue is unmasked, and a third carboxylic acid, originally hydrogen bonded to the acid/base catalytic residue, assumes catalytic importance. The net result would be a shift of the profile to higher pH, which is what is observed here and was also seen for an "acidic" xylanase upon mutation of one of the acid/base pair of amino acids (*35*). The converse shift in pH optimum was seen upon introducing a second carboxylic acid to the *B. circulans* xylanase (*34*). Regardless of the source of the apparent additional ionization, these unusual effects on the pH profile of the mutant enzyme are consistent with E160 having a significant role in catalysis as the acid/base catalytic residue. Additionally, should reverse protonation acid catalysis operate for XynB, then on the basis of the work described here, E160 is expected to be the member of the acid/base catalytic diad which acts directly to deliver a proton to the glycosidic oxygen.

Another important consequence of removal of the acid/base catalytic residue would be that the two steps in catalysis, formation and hydrolysis of the xylosyl−enzyme, would be

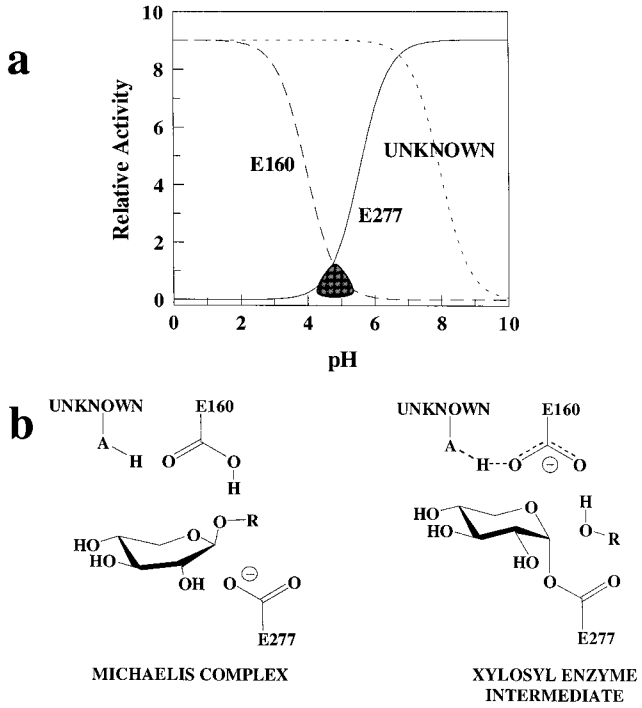

FIGURE 11: (a) Simulated activity profiles for the proposed acid catalysis involving reverse protonation of active site residues. The shaded area encompassed by the ionizations of the "direct" acid/base catalytic residue (E160, dashed line) and the nucleophile (E277, solid line) reflects the ionization state of the catalytically active Michaelis complex (shown below in panel b). On deletion of the "direct" acid/base catalytic residue, the ionization of a third active site residue is revealed (dotted line), and the pH optimum is shifted to a higher value. (b) The protonation states of three ionizable residues are shown for the Michaelis complex and the xylosyl−enzyme intermediate. The putative strong hydrogen bond is formed within the acid/base catalytic diad. The E160 residue is shown here as functioning as the "direct" acid/base residue but may instead be the "auxiliary" acid/base catalytic residue indicated here by A.

affected differently by the removal of this key group. The deglycosylation step should be slowed equally for all substrates of the same glycone as a consequence of removal of general base assistance. On the other hand, the effect on the glycosylation step would be dependent upon the need for general acid catalytic assistance for the departure of the aglycone in each case. Such behavior has been seen in several other glycosidases (*19*−*22*, *30*) and allows one to probe the importance of both forms of catalysis. The appreciable residual activity and the chemical rescue (vide infra) strongly suggest that the E160A mutant enzyme is properly folded. Moreover, the extent to which the catalytic activity of $XynBH_6$(E160A) is impaired is strongly dependent on the leaving group pK_a of the substrate (Table 1). Conveniently, steady-state determinations of the second-order rate constants, k_{cat}/K_m, permit access to information regarding the first irreversible step on the reaction coordinate; the xylosylation step. From the complete data set for $XynBH_6$, it is already known that there is an unexpected deviation from linearity (see the preceding paper). In the plot containing the limited data set shown here (Figure 7a), that deviation is likely masked in the data shown here by the absence of sufficient data points. Thus direct comparisons between data outlined in Table 1 for the wild-type and mutant enzyme must be made with caution. For the mutant enzyme, the large, negative slope of the Brønsted plot of log(k_{cat}/K_m) against pK_a ($\beta_{lg} = -1.4$) is consistent with the xylosylation step being the first irreversible process on the reaction coordinate. The $\beta_{lg(kcat/Km)}$ value for the E160A mutant ($\beta_{lg} = -1.4$) as compared to that of the wild-type enzyme determined in the preceding paper ($\beta_{lg(kcat/Km)} = -0.97$) indicates that there is a greater net negative charge developed on the glycosidic oxygen in the xylosylation transition state for the acid/base catalytic mutant enzyme as compared to that of the wild-type enzyme. Indeed, for substrates bearing poor leaving groups (pK_a > 7), this effect is pronounced, and for the poorest substrate studied here, the second-order rate constant for the mutant enzyme is smaller by 5 orders of magnitude than that found for the wild-type enzyme. Such a marked difference likely stems from the absence of effective proton donation to the glycosidic oxygen that would act to neutralize the developing negative charge. This interpretation is certainly consistent with the known deleterious effects of deletion of the acid/base catalytic residue on the activity in acid/base catalyst mutants of the *Bacillus circulans* xylanase (*22*) on xylan and of hen egg white lysozyme on peptidoglycan (*36*).

Previous kinetic studies using aryl glycosides with glycosyl hydrolases in which the acid/base catalytic residue has been mutated have revealed that, for substrates bearing reasonably good leaving groups, the deglycosylation step is slowed to a greater extent than the glycosylation step and that deglycosylation is rate-limiting. However, in this study, the opposite appears to be the case. The Brønsted plot of log(k_{cat}) for the hydrolysis of a series of aryl xylosides by the wild-type enzyme against pK_a of the leaving group reveals essentially no dependence on leaving group ability in the pK_a range of 5−8 (Figure 7b and the preceding paper). This suggests that the dexylosylation step is rate-limiting for these substrates, and indeed, studies outlined in the preceding paper have confirmed this view. With the $XynBH_6$(E160A) mutant, the Brønsted plot reveals a strong dependence on leaving group ability ($\beta_{lg} = -0.65$), suggesting that the xylosylation step is rate-determining (Figure 7b), at least for the poorer substrates (p$K_a \geq 7$). However, the slope (β_{lg}) of the plot of log(k_{cat}) versus pK_a is less negative than that of the plot of log(k_{cat}/K_m) vs pK_a ($\beta_{lg} = -0.97$). Indeed, if the rate-determining step is the xylosylation step for all substrates with the E160A mutant enzyme, one would expect these slopes to be of the same value. The simplest explanation for the apparent difference in slopes is that for the most highly activated substrates the deglycosylation step has become rate-limiting; thus, the rates measured for these substrates no longer reflect the glycosylation step and are therefore somewhat lower than would otherwise be the case. This has the consequence of skewing the plot of log(k_{cat}) for the E160A mutant enzyme. In reality, the plot of log(k_{cat}) versus pK_a for the mutant enzyme is probably downward-curving, as with that for the wild-type enzyme. If the dexylosylation step is at least partially rate-determining for these highly activated substrates with the E160A mutant enzyme, then the addition of competitive nucleophiles into the reaction mixture should result in an increase in the rate of their cleavage.

Effect of Competitive Nucleophiles on Rates of Hydrolysis by XynBH$_6$(E160A). The formation of β-azide products by suitable mutants has been shown to be a useful diagnostic tool for identifying the acid/base catalytic residue of retaining

β-glycosidases. Typically, the wild-type enzymes do not generate azide products under identical conditions (*20*, *30*). Consequently, the observation that both the $XynBH_6$ and the Glu160Ala mutant enzyme yield β-azide products is ambiguous and forces careful analysis of the kinetic behavior of these enzymes in the presence of exogenous nucleophiles.

In addressing the possible cause for the increases in the rates of hydrolysis of 3,4DNPX by both $XynBH_6$ and $XynBH_6$(E160A) upon inclusion of azide in the reaction mixtures, consideration must be made as to which step is rate-determining. For the wild-type enzyme acting on 3,4DNPX, the rate-determining step is clearly dexylosylation (vide supra and the preceding paper), while for $XynBH_6$(E160A), the Brønsted plot of log(k_{cat}) against pK_a of the phenol leaving group would suggest that xylosylation is partially rate-determining. There is some evidence, outlined above, stemming from the inequality of $\beta_{lg(kcat/Km)}$ and $\beta_{lg(kcat)}$, that xylosylation is, at best, only partially rate-limiting for $XynBH_6$(E160A), at least with the most activated substrates (p$K_a \approx 5$). If the xylosylation step were entirely rate-determining for the mutant enzyme, we would expect at most only a very small effect (<2-fold) from added nucleophiles on the rate of hydrolysis of 3,4DNPX that may result from the anion assisting that step by acting as a general acid/base catalyst (*20*).

The 8-fold increase in the rate of cleavage of 3,4DNPX upon inclusion of azide observed with the mutant enzyme clearly shows that the deglycosylation step is substantially rate-limiting for $XynBH_6$(E160A) with this substrate, consistent with our interpretation of the Brønsted plots. The increase in rate observed with the wild-type enzyme is surprising and suggests that azide can intercept the xylosyl−enzyme intermediate despite the presence of the acid/base catalytic group. This is in marked contrast to previous studies with other wild-type glycosidases (*20*, *30*), where the absence of any effect of added azide was rationalized on the basis of the charge of the carboxylate side chain of the acid/base residue screening the active site from the negatively charged azide. Clearly, charge screening does not prohibit azide from competing with water for the $XynBH_6$ xylosyl−enzyme intermediate. Why the xylosyl−enzyme studied here is more susceptible to attack by azide than the glycosyl−enzyme intermediates from *Agrobacterium* sp. β-glucosidase or the xylanase from *Cellulomonas fimi* is unclear. One possible explanation, which will be expanded upon in the conclusion is that this may be a consequence of the active site architecture required for glycosidases using reverse protonation.

The absence of any increase in k_{cat}/K_m implies that azide has no effect on the xylosylation step. Indeed, insensitivity of k_{cat}/K_m to azide concentration has been observed in such studies previously (*20*, *30*). The increase in k_{cat} upon addition of azide and the formation of a β-xylosyl azide product is consistent with azide being a more effective nucleophile than water in reacting with the xylosyl−enzyme intermediate. The observed increase in K_m as a function of azide concentration is also consistent with this interpretation since by selectively speeding the deglycosylation step the steady-state concentration of the xylosyl−enzyme intermediate is decreased.

The observed increase in k_{cat} with increasing azide concentration is similar to that observed with the acid/base mutant (Glu127Ala) of the *Bacillus circulans* xylanase (*22*) (8-fold) and also the family 39 β-xylosidase from *Bacillus stearothermophilus* (*19*). Most other studies have revealed a much greater effect of azide on rate (up to several 100-fold), but in these cases, the rate-determining step was, in all instances, the deglycosylation step. The moderate increase in k_{cat} is therefore consistent with k_{cat} being governed primarily by the xylosylation step, as evidenced by sloped Brønsted plots of log(k_{cat}) versus pK_a. Indeed, the limiting value of k_{cat} for the $XynBH_6$(E160A) catalyzed cleavage of 3,4DNPX in the presence of high concentrations of azide likely reflects only the xylosylation step (k_2). Using this limiting value for k_{cat} and also disregarding the data for 2,5DNPX (which has not been measured in the presence of high concentrations of azide), we measured a $\beta_{lg(kcat)}$ value of −1.03. This value is markedly different from that measured using the value of k_{cat} for the hydrolysis of 3,4DNPX in the absence of azide ($\beta_{lg(kcat)} = -0.65$) and is very similar to the $\beta_{lg(kcat/Km)}$ value (−0.97) measured for $XynBH_6$(E160A). The close agreement between the $\beta_{lg(kcat/Km)}$ value and this "corrected" $\beta_{lg(kcat)}$ value suggests that the rate-determining step for the cleavage of 3,4DNPX in the presence of azide is the xylosylation step and provides further evidence that the rate-determining step for these activated substrates with the $XynBH_6$(E160A) mutant enzyme is, at least in part, the dexylosylation step.

Consequently, the leveling off of k_{cat} as the azide concentration is increased likely arises from the xylosylation step becoming solely, rather than partially, rate-determining. The effects that are observed lend further support for the assignment of Glu160 as the catalytic acid/base residue.

CONCLUSIONS

The affinity label NBX inactivates $XynBH_6$ according to pseudo-first-order kinetics and stoichiometrically labels a completely conserved carboxyl group within the active site of the enzyme. This residue, Glu160, on the basis of the kinetic studies within this investigation, can be assigned as the catalytic acid/base residue within XynB. This supports the observations of Bravman et al. (*19*) and by extension allows the unambiguous assignment of this highly conserved residue within all members of family 39 of glycoside hydrolases as the catalytic acid/base residue. This study also suggests that despite the early failures of *N*-bromoacetyl saccharides for the specific labeling of the acid/base catalytic residue (*12*, *14*), these compounds may be reasonably specific for the acid/base catalytic residue and can certainly provide a valuable lead. Additionally, through detailed kinetic analyses, it is apparent that the catalytic acid/base residue in XynB is of great importance for the hydrolysis of substrates that require acid catalysis and it also facilitates, to a lesser extent, the hydrolysis of substrates with good leaving groups not requiring efficient acid catalysis. Additionally, several lines of reasoning support reverse protonation acid catalysis for the wild-type XynB.

First, the upward shift of the bell-shaped pH dependence observed for the XynB upon site-directed deletion of the carboxyl side chain of the catalytic acid/base residue is similar to that observed for the acidic xylanase C from *Aspergillus kawachii*. In that case, Fushinobu et al. were able to convert the acidic xylanase C into an "alkaline" xylanase by mutating the carboxyl group closely associated with the acid/base catalytic residue of that enzyme to a neutral residue (*35*). Joshi et al. accomplished the opposite by converting the "alkaline" *Bacillus circulans* xylanase into an acidic

xylanase (*34*). In that case, mutation of the partner of the acid/base catalytic residue, Asn35, to an Asp residue resulted in the bell-shaped pH profile being shifted to a lower pH optimum. This N35D mutant xylanase was shown, by site-specific measurements of the pK_a values of the catalytic residues by ^{13}C-nmr spectroscopy, to use acid catalysis involving reverse protonation. The three-dimensional structure of this N35D mutant xylanase (*34*) revealed significant similarity to the X-ray structures of several acidic xylanases (*35*, *37*, *38*) in that the acid/base catalytic residue formed a short hydrogen bond with its partner.

Second, the Brønsted plot for the acid/base catalytic mutant E160A indicates that the mutation of this residue results in the xylosylation step being preferentially slowed. This unexpected result can be rationalized on the basis of the enzyme using acid catalysis involving reverse protonation of active site residues. It has been argued that the glycosyl−enzyme intermediate and flanking transition states for the family 11 "acidic" xylanases are stabilized by the formation of a short strong hydrogen bond between the acid/base catalytic residue and its partner. Such a strong hydrogen bond, however, does not exist in the active free enzyme where both of these carboxyl groups are protonated. Consequently, deletion of the acid/base residue would remove this hydrogen bond, thereby destabilizing the intermediate and the flanking transition states to a similar extent. The net result would be an increase in the activation free energy for the xylosylation step relative to that of the dexylosylation step.

Third, the weak azide effects observed with the wild-type enzyme, although unexpected, can again be rationalized on the basis of a reverse protonation. As discussed earlier, the three-dimensional structure of the glycosyl−enzyme intermediate of the acidic N35D *B. circulans* xylanase indicates that the acid/base catalytic residue and its close partner form a very tight hydrogen bond (*34*). Such intimate contact would act to disperse the negative charge of the catalytic base residue, thereby reducing the charge shielding of the xylosyl−enzyme intermediate, possibly allowing anions to enter the active site. The elucidation of a three-dimensional structure of one of the family 39 xylosidases should prove to be of considerable interest in addressing the possibility, outlined here, of a catalytic mechanism for XynB involving reverse protonation.

ACKNOWLEDGMENT

We thank Dr. Shouming He for technical assistance with the MS work, Dr. Gregory Zeikus for the *xynB* gene, Dr. Lothar Ziser, and Lloyd Mackenzie for providing some of the substrates used in this study.

REFERENCES

1. McCarter, J., and Withers, S. G. (1994) *Curr. Op. Struct. Biol. 4*, 885−892.
2. Coutinho, P. M., and Henrissat, B. (1999) Carbohydrate-Active Enzymes, http://afmb.cnrs-mrs.fr/~cazy/CAZY/index.html.
3. Mackenzie, L. F., Wang, Q., Warren, R. A. J., and Withers, S. G. (1998) *J. Am. Chem. Soc. 120*, 5583−5584.
4. McCarter, J. D., and Withers, S. G. (1996) *J. Am. Chem. Soc. 118*, 241.
5. Vocadlo, D. J., Mayer, C., He, S., and Withers, S. G. (2000) *Biochemistry 39*, 117−126.
6. Howard, S., He, S., and Withers, S. G. (1998) *J. Biol. Chem. 273*, 2067−2072.
7. Withers, S. G., and Aebersold, R. (1995) *Protein Sci. 4*, 361−372.
8. Miao, S., Ziser, L., Aebersold, R., and Withers, S. G. (1994) *Biochemistry 33*, 7027−32.
9. McCarter, J. D., Yeung, W., Chow, J., Dolphin, D., and Withers, S. G. (1997) *J. Am. Chem. Soc. 119*, 5792−5797.
10. Vocadlo, D. J., Davies, G. J., Laine, R., and Withers, S. G. (2001) *Nature 412*, 835−838.
11. Havukainen, R., Törrönen, A., Laitinen, T., and Rouvinen, J. (1996) *Biochemistry 35*, 9617−9624.
12. Yariv, J., Wilson, K., Hildesheim, J., and Blumberg, S. (1971) *FEBS Lett. 15*, 24−26.
13. Keresztessy, Z., Kiss, L., and Hughes, M. A. (1994) *Arch. Biochem. Biophys. 315*, 323−330.
14. Black, T. S., Kiss, L., Tull, D., and Withers, S. G. (1993) *Carbohydr. Res. 250*, 195−202.
15. Tull, D., Burgoyne, D. L., Chow, D. T., Withers, S. G., and Aebersold, R. (1996) *Anal. Biochem. 234*, 119−125.
16. White, A., Tull, D., Johns, K., Gilkes, N. R., Withers, S. G., and Rose, D. R. (1996) *Nat. Struct. Biol. 3*, 149−154.
17. MacLeod, A. M., Lindhorst, T., Withers, S. G., and Warren, R. A. (1994) *Biochemistry 33*, 6371−6376.
18. Howard, S., and Withers, S. G. (1998) *Biochemistry 37*, 3858−3864.
19. Bravman, T., Mechaly, A., Shulami, S., Belakhov, V., Baasov, T., Shoham, G., and Shoham, Y. (2001) *FEBS Lett. 495*, 115−119.
20. Wang, Q., Trimbur, D., Graham, R., Warren, R. A., and Withers, S. G. (1995) *Biochemistry 34*, 14554−14562.
21. Viladot, J.-L., de Ramon, E., Durany, O., and Planas, A. (1998) *Biochemistry 37*, 11332−11342.
22. Lawson, S. L., Wakarchuk, W. W., and Withers, S. G. (1997) *Biochemistry 36*, 2257−2265.
23. Thomas, E. W. (1977) *Methods Enzymol. 46*, 362−368.
24. Onodera, K., and Kitaoka, S. (1960) *J. Org. Chem 25*, 1322−1325.
25. Kempton, J. B., and Withers, S. G. (1992) *Biochemistry 31*, 9961−9969.
26. Tull, D., and Withers, S. G. (1994) *Biochemistry 33*, 6363−6370.
27. Leatherbarrow, R. J. (1996) *GraFit 3.09b*, Erithacus Software Ltd., Surrey, U.K.
28. Gyorgydeak, Z., and Szilagyi, L. (1986) *Liebigs. Ann. Chem.*, 1393−1397.
29. Vocadlo, D. J., MacKenzie, L. F., He, S., Zeikus, G. J., and Withers, S. G. (1998) *Biochem. J. 335*, 449−455.
30. MacLeod, A. M., Tull, D., Rupitz, K., Warren, R. A. J., and Withers, S. G. (1996) *Biochemistry 35*, 13165−13172.
31. Henrissat, B., Callebaut, I., Fabrega, S., Lehn, P., Mornon, J.-P., and Davies, G. (1995) *Proc. Natl. Acad. Sci. U.S.A. 92*, 7090−7094.
32. Fersht, A. R. (1976) *Enzyme Structure and Mechanism*, 2 ed., W. H. Freeman & Co., New York.
33. Mock, W. L., and Stanford, D. J. (1996) *Biochemistry 35*, 7369−7377.
34. Joshi, M. D., Sidhu, G., Pot, I., Brayer, G. D., Withers, S. G., and McIntosh, L. P. (2000) *J. Mol. Biol. 299*, 255−279.
35. Fushinobu, S., Ito, K., Konno, M., Wakagi, T., and Matsuzawa, H. (1998) *Protein Eng. 11*, 1121−1128.
36. Malcolm, B. A., Rosenberg, S., Corey, M. J., Allen, J. S., de Baetselier, A., and Kirsch, J. F. (1989) *Proc. Natl. Acad. Sci. U.S.A. 86*, 133−137.
37. Torronen, A., and Rouvinen, J. (1995) *Biochemistry 34*, 847−856.
38. Krengel, U., and Dijkstra, B. (1996) *J. Mol. Biol. 263*, 70−78.
39. Lee, Y.-E., and Zeikus, J. G. (1993) *J. Gen. Microbiol. 139*, 1235−1243.
40. Luethi, E., Love, D. R., McAnulty, J., Wallace, C., Caughey, P. A., Saul, D., and Bergquist, P. L. (1990) *Appl. Environ. Microbiol. 56*, 1017−1024.
41. Scott, H. S., Anson, D. S., Orsborn, A. M., Nelson, P. V., Clements, P. R., Morris, C. P., and Hopwood, J. J. (1991) *Proc. Natl. Acad. Sci. U.S.A. 88*, 9695−9699.
42. Stoltzfus, L. J., Sosa-Pineda, B., Moskowitz, S. M., Menon, K. P., Dlott, B., Hooper, L., Teplow, D. B., Shull, R. M., and Neufeld, E. F. (1992) *J. Biol. Chem. 267*, 6570−6575.
43. Clarke, L. A., Nasir, J., McDonald, H., Applegarth, D. A., Hayden, M. R., and Toone, J. (1994) *Genomics 24*, 311−316.

BI020078N